

# Thermal Analysis of Polyamide Blends as Obtained by Reactive Melt-Extrusion: Influence of Blend Composition on Crystallization and Melting Behavior

K. L. L. EERSELS, G. GROENINCKX

Catholic University of Leuven, Department of Chemistry, Laboratory for Macromolecular Structural Chemistry, Celestijnenlaan 200 F, 3001 Heverlee, Belgium

Received 28 December 1995; accepted 24 August 1996

**ABSTRACT:** Polyamide blends composed of PA 46 and PA 6I were melt-mixed using a double-screw extruder, and the obtained compounds were subsequently processed by injection molding. The blend materials obtained were found to have undergone transamidation processes during the extrusion and injection-molding operations which alter the crystallization and melting behavior. The variation in thermal behavior is strongly dependent on the change in the average sequence length of the crystallizable component in the copolymer formed; it is affected by the compounding and processing conditions and by the blend composition. The influence of every melt-processing step on the crystallization and melting behavior of the blends was investigated by thermal analysis using extruded, injection-molded, and solution-prepared blends. © 1997 John Wiley & Sons, Inc. *J Appl Polym Sci* **63**: 573–580, 1997

**Key words:** polyamides; blends; reactive extrusion; transamidation; copolyamides

## INTRODUCTION

In the growing area of reactive extrusion of non-miscible polymers, one of the main objectives is to reach compatibilization for the blend systems.<sup>1</sup> In this respect, functionalized polymers which can undergo chemical reactions during melt-mixing are being used.<sup>2–4</sup> The formation of block or graft copolymers by this way will lower the interfacial tension and will result in a finer phase dispersion and better stability against coalescence. However, it is important to realize that another class of reactive polymers is formed by the polycondensates. Polycondensates such as polyesters, polycarbonates, polyethers, and polyamides are known as being very reactive during melt-mixing.<sup>5–8</sup> The transreaction processes occurring in polyconden-

sates can give rise to a different molecular weight distribution in homopolymers<sup>9,10</sup> or can lead to the formation of block copolymers if two different homopolycondensates are used as blend components.<sup>11–13</sup>

In a previous article,<sup>14</sup> it was shown that melt-mixing of two different polyamides at elevated temperatures results in transamidation processes between the blend components. It was also demonstrated how transamidation processes can affect the crystallization kinetics and the melting properties of polyamide blends composed of an amorphous, aromatic polyamide (PA 6I) and a semicrystalline, aliphatic polyamide (PA 46). PA 46 and PA 6I are fully miscible over the whole composition range.<sup>14</sup> The main objective of the previous article was to demonstrate the influence of the mixing temperature and the mixing time on the melting and crystallization behavior of PA 46/PA 6I blends at a constant blend composition. All the experiments were performed on a laboratory scale by means of a mini-mixer/extruder.

---

Correspondence to: G. Groeninckx  
Contract grant sponsor: DSM Research, Geleen, The Netherlands

© 1997 John Wiley & Sons, Inc. CCC 0021-8995/97/050573-08

In this work, upscaling was performed to determine to what extent the previous results are reproducible when the blends are prepared using a large-scale double-screw extruder. This is a very important step with respect to the applicability of this concept for the preparation of block copolyamides during melt-extrusion. In contrast to the previous article, the extrusion conditions remain unchanged but the blend composition was altered. After the melt-extrusion, injection-molded samples were prepared from the compounded blends. All blend compositions were systematically studied by thermal analysis, and a comparison was made with blend compositions which were prepared by coprecipitation from a common solvent.

## EXPERIMENTAL

### Blend Components

The aliphatic polyamide (PA 46) is a condensation product of 1,4-diaminobutane and adipic acid. The aromatic polyamide (PA 6I) is a condensation product of 1,6-diaminohexane and isophthalic acid. All polyamides used in this study are commercial grades without additives. The molecular characterization was presented elsewhere.<sup>14</sup>

### Blend Preparation

#### *Solution-prepared Blends*

Blends of PA 46 and PA 6I were prepared at several compositions via the solution/coprecipitation method; formic acid was used as a common solvent, and deionized water, as a nonsolvent.

#### *Melt-mixed Blends*

Blends of PA 46 and PA 6I were compounded at several compositions by melt-extrusion using a ZSK 25 twin-screw extruder. The temperature of the melt was 315°C. The extrusion time was determined by means of a masterbatch; the average residence time in the extruder was about 2.5 min.

#### *Injection-molded Blends*

The blend compounds obtained by melt-extrusion were injection-molded (IM) into bars on a Battenfield machine. The melt-residence time during the injection-molding process was about 1–1.5 min.

### Calorimetric Measurements

The crystallization and melting behavior of the blends was studied using a Perkin-Elmer Delta Series DSC 7. Liquid nitrogen was used as a cooling agent and the DSC measurements were performed under a nitrogen atmosphere.

The dynamic crystallization temperature of the blends was measured by cooling the samples from 300 to 200°C at a cooling rate of 10°C/min. The crystallized blends were then subsequently heated up to 320°C at 10°C/min to determine the corresponding melting temperature. Quench-cooling experiments were performed by quenching the samples from 300 to –78°C into cooled isopropanol. The corresponding glass transition temperature of the quenched samples was measured by heating them from 10 to 200°C at 20°C/min. Subsequently, the samples were cooled from 200 to 10°C and then heated for a second time to detect  $T_g$  changes, due to possible crystallization processes during the first heat treatment.

## RESULTS AND DISCUSSION

### Crystallization and Melting Behavior of PA 46/PA 6I Blends

From a previous article on PA 46/PA 6I blends prepared using a mini-extruder, it clearly appeared that the thermal behavior of the crystallizable component PA 46 is influenced by transreaction processes with the amorphous aromatic component PA 6I during the melt-mixing process of the blend.<sup>14</sup> The extent of the transreaction processes between PA 46 and PA 6I, and, as a consequence, the average crystallizable segment length of PA 46 in the copolymers formed, can be controlled by the extrusion temperature and the extrusion time.<sup>15,16</sup> Under constant extrusion conditions, it will be shown that the initial blend composition strongly influences the crystallization and melting behavior of PA 46 in the blends.

Figure 1 shows the decrease of the crystallization temperature for the various blend compositions as obtained by the different modes of preparation. It appears from the crystallization peak temperatures that transreaction processes have also occurred when the blends are compounded using a large scale ZSK double-screw extruder (residence time: ~ 2.5 min). The crystallization peak temperature changes to a large extent when the blend composition is changed. The blend with 30% (w/w) PA 46 crystallizes around 240°C when

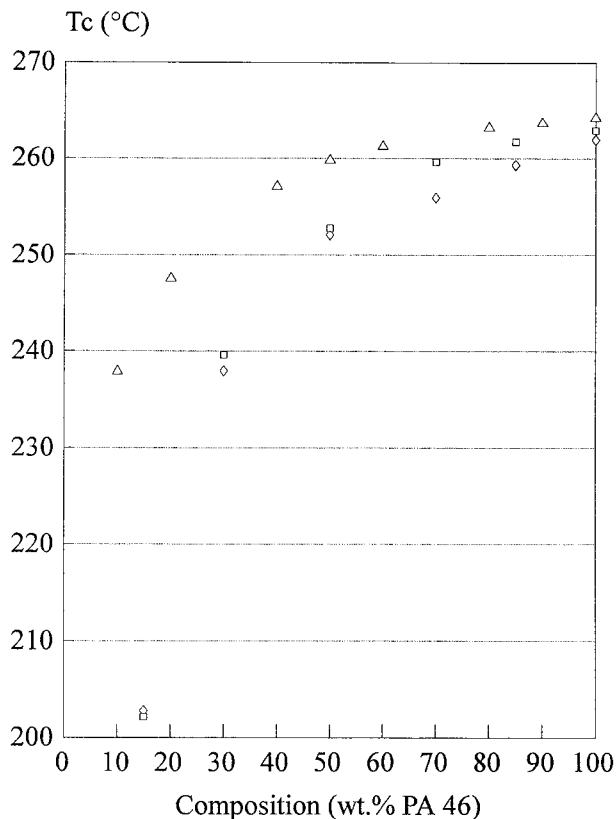


**Figure 1** Influence of the blend composition on the peak crystallization temperature of PA 46/PA 6I blends during cooling from the melt ( $-10^{\circ}\text{C}/\text{min}$ ): ( $\Delta$ ) solution-prepared blends; ( $\square$ ) extruded blends; ( $\diamond$ ) IM blends.

the blend is cooled from the melt at  $10^{\circ}\text{C}/\text{min}$ . This is more than  $20^{\circ}\text{C}$  below the crystallization peak temperature of pure PA 46. It can also be seen that the blend with only 15% (w/w) PA 46 is still able to crystallize around  $200^{\circ}\text{C}$ ; however, the observed crystallization peak is becoming very broad, indicating a low crystallization rate.

Our previous article described to what extent the crystallization rate of the block copolyamides formed is reduced by the decreasing length of the crystallizable PA 46 sequences.<sup>14</sup> The average PA 46 sequence length is determined by the number of transreaction processes between the two chemically different polyamides and is dependent on the extrusion temperature and the extrusion time. However, the number of transamidation reactions between PA 46 and PA 6I is also dependent on the volume fraction of both blend components. An excess of PA 6I in the blends will result in a fast conversion of homopolyamide 46 into a segmented block copolymer with rather short crystallizable

sequences after a short extrusion time; this will lead to a large decrease of the crystallization temperature of PA 46 in the blends. When PA 6I is only present in a low concentration, a short extrusion time will affect the crystallizable PA 46 molecules only to a small extent, resulting in a slight decrease of the crystallization temperature (i.e., crystallization rate).

The decrease in crystallization temperature of the melt-mixed blends is much more pronounced compared with the solution-prepared blends. In the solution-prepared blends, the decrease in crystallization kinetics of PA 46 can be ascribed mainly to the lower chain mobility of PA 46 due to the presence of stiff aromatic polymer chains of PA 6I. Moreover, addition of aromatic PA 6I results in a higher  $T_g$  of the polyamide blend. Melt-mixing of PA 46/PA 6I blends results in an additional limitation of PA 46 chain mobility due to chemical bonding of crystallizable PA 46 chain segments to noncrystallizable PA 6I sequences. This causes a further decrease of the crystallization kinetics of PA 46, resulting in an even lower crystallization temperature.

It has to be emphasized that the measurement of the dynamic crystallization temperature of all blends always implies an additional melt residence time between the melting and the crystallization of the blends which cannot be avoided. During this melt-residence time (5–7 min at a scanning rate of  $10^{\circ}\text{C}/\text{min}$ ), transreaction processes will occur and, hence, will lower the crystallization temperature of the blends. This is also the case for the blends obtained by coprecipitation, which means that these blends have also undergone some transreaction processes at the onset of crystallization.

The blends obtained by extrusion followed by injection molding reveal a similar crystallization behavior but the crystallization peak temperatures of the IM blends are slightly below those of the extruded blends. This can easily be understood if an additional melt-residence time of 1–1.5 min during the injection-molding process is taken into account; the transamidation processes proceeding during this time interval result in slower crystallization kinetics of the injection-molded blends as a consequence of the shorter crystallizable sequences of PA 46.

Similar remarks can be made when the melting temperatures of the crystallized blends are compared to each other (Fig. 2). The melting temperature of the extruded blend with 30% (w/w) PA 46 is about  $274^{\circ}\text{C}$ , almost  $20^{\circ}\text{C}$  below the melting

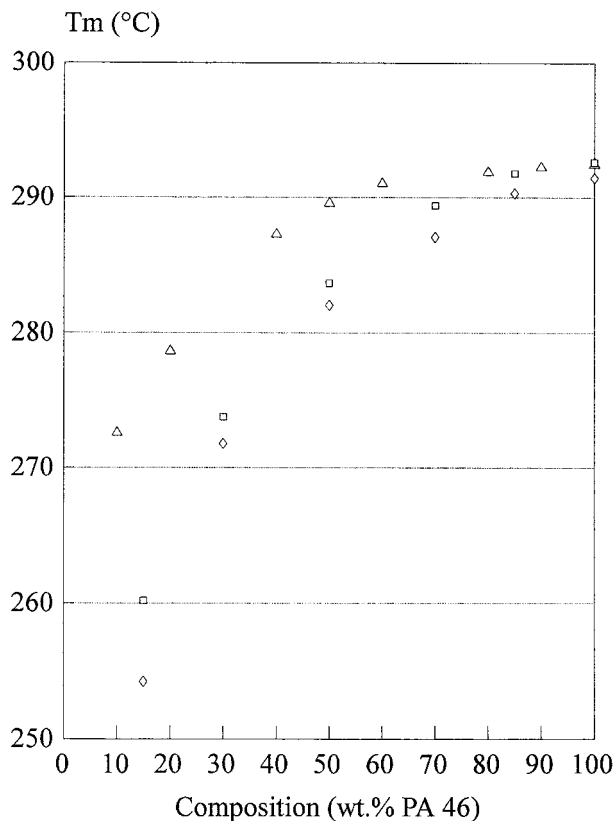


**Figure 2** Influence of the blend composition on the peak melting temperature of PA 46/PA 6I blends after slow cooling from the melt (10°C/min): (△) solution-prepared blends; (□) extruded blends; (◇) IM blends.

temperature of pure PA 46; a very broad and weak melting domain is found around 260°C for the blend with 15% (w/w) PA 46. From Figure 2, it also can be seen that the melting temperatures of the injection-molded samples are again just below those of the extruded blends but far below those of the solution-prepared blends. The correlation of the melting temperature with the semicrystalline morphology of the copolymers formed during melt-mixing was investigated using WAXS, SAXS, and TEM. It will be the subject of a further publication.

Besides dynamic crystallization, isothermal crystallization experiments at 268°C were also performed for the various blend compositions. Figure 3 clearly shows how the crystallization time increases as the blend composition is changed to a higher content of PA 6I. The blends with 30% PA 46 and less do not show any crystallization exotherm. This illustrates once more the slower crystallization kinetics of PA 46 in the blends with an increasing content of PA 6I, due

mainly to the occurrence of transamidation processes in the polyamide blends.

### Thermal Behavior of Quench-cooled Blends

#### Cold-crystallization of Quench-cooled Blends

The occurrence of a cold-crystallization process during the first heat treatment after quench-cooling of the blends is an interesting phenomenon which allows us to have a better insight in the crystallization kinetics of the blends. Cold-crystallization occurs when the crystallization rate is too slow to allow complete crystallization at high cooling rates from the melt (e.g., during quenching). The appearance of a cold-crystallization peak during heating from room temperature of a quenched sample indicates slower crystallization kinetics of the blend. Such experiments were performed for the quenched extruded blends, the quenched injection-molded blends, the original injection-molded blends (i.e., blends cooled in the mold), and the quenched solution-prepared blends.

In Figure 4, one can see that cold-crystallization is clearly observed for several compounded blends, containing 50% PA 6I and more, when these blends are quenched from the melt. However, cold-crystallization is already observed for the quenched IM blends containing only 30% PA 6I (Table I). This is due to the additional melt-residence time during IM compared to extruded blends; crystallizable sequences of PA 46 become shorter with the additional IM time, and as a consequence, crystallization becomes more difficult. This is another indication that transamidation

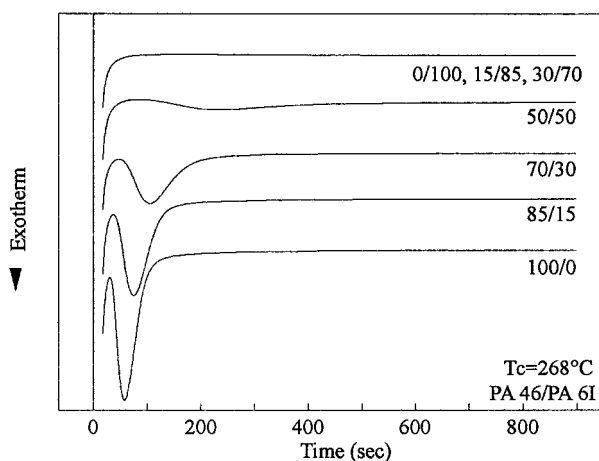


**Figure 3** Influence of the blend composition on the isothermal crystallization behavior of the extruded PA 46/PA 6I blends at 268°C.

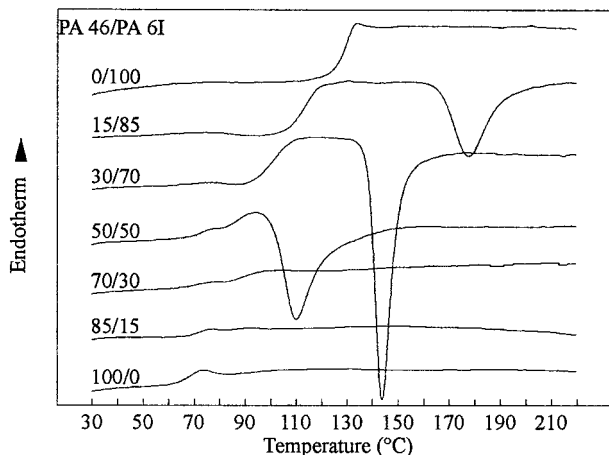


**Figure 4** Representative thermograms for the various compositions of the extruded blends after quench-cooling from the melt.

processes are proceeding as a function of the melt-processing time.

From Table I, it can also be seen that complete crystallization of PA 46 in the solution-prepared blends containing 50% PA 6I is still possible, even during quench-cooling. This has to be ascribed to a lower amount of transamidation reactions due to a shorter melt-residence time. In fact, the only melt-residence time is the melting process before quench-cooling, which is 1 min.

The occurrence of a cold-crystallization peak also depends on the cooling rate, as already mentioned. The quenched IM blends reveal cold-crystallization for the blends containing 30% PA 6I and more (Table I). However, if the blends are cooled in the mold (i.e., a lower cooling rate), cold-crystallization occurs only for the blends with 70%

PA 6I and more. Moreover, it could be seen from the DSC scans that samples taken from the edge of an IM bar show a stronger cold-crystallization process compared with samples taken from the center of the IM bar. This is not surprising since the cooling rate is higher at the edge of the bar compared with that in the center of the bar.

#### **Change of the Glass Transition Temperature as a Function of Blend Composition and Thermal History**

The glass transition temperature of miscible polymer blends is largely determined by the composition of the amorphous phase and is given by the equation of Fox:

$$\frac{1}{T_g} = \frac{\omega_1}{T_{g1}} + \frac{\omega_2}{T_{g2}}$$

In case of random copolymers, the glass transition is given by the equation of Gordon–Taylor:

$$(T_g - T_{g1})\omega_1 + K(T_g - T_{g2})\omega_2 = 0$$

The blends which were compounded by melt-extrusion and the blends which were additionally processed by injection molding were all quenched from the melt. The first heating scan was recorded in order to measure the  $T_g$  of the quenched samples. Figure 5 shows how the  $T_g$  of the compounded blends is shifting to a higher temperature with increasing PA 6I content. Besides the  $T_g$ , cold-crystallization is also observed for several blend compositions, as discussed in the previous section (Fig. 4). The occurrence of cold-crystalli-

**Table I** The Influence of Blend Composition, Thermal History, and Cooling Conditions of PA 46/PA 6I Blends on the Occurrence of Cold-crystallization Processes

Series	Cold-crystallization Temperature (°C) as a Function of the Blend Composition (PA 46/PA 6I)								
	70/30	60/40	50/50	40/60	30/70	20/80	15/85	10/90	0/100
Injection-molded (original)	—	—	—	n.d.	142	n.d.	176	n.d.	—
Solution-prepared (quenched)	—	—	—	124	n.d.	156	n.d.	183	—
Compounded (quenched)	—	—	115	n.d.	145	n.d.	183	n.d.	—
Injection-molded (quenched)	92	n.d.	113	n.d.	147	n.d.	178	n.d.	—

—: absence of cold-crystallization; n.d.: no experimental data.

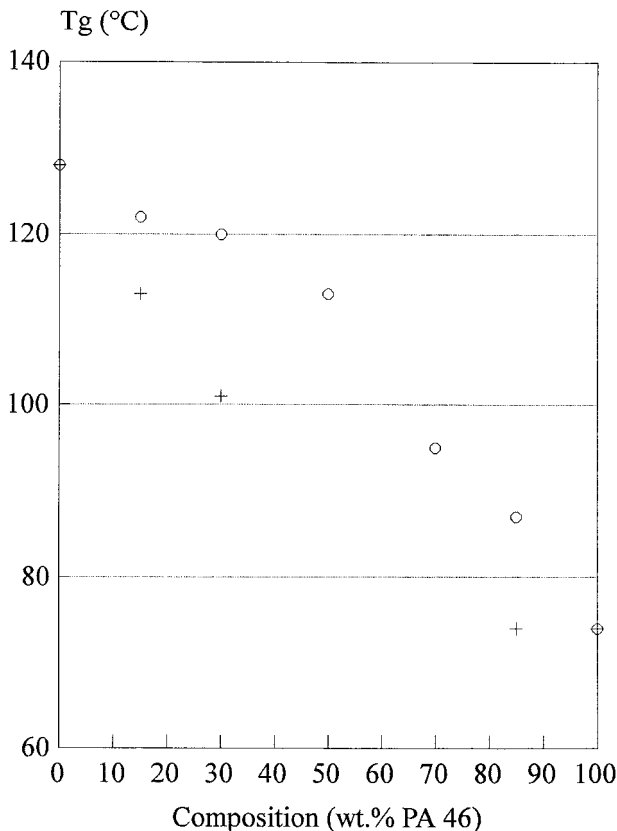


**Figure 5** Glass transition temperatures of extruded PA 46/PA 6I blends as a function of the blend composition: (+) quench-cooled blends; (○) annealed blends.

zation during the first heating scan sometimes hinders the determination of the  $T_g$  (missing data points for some blend compositions in Figs. 5 and 6). Figure 5 also reveals that the cold-crystallization process increases the  $T_g$  to a large extent; the cold-crystallization process extracts crystallizable PA 46 from the miscible amorphous phase which then becomes richer in PA 6I. Moreover, additional crystallization of the blends implies less chain mobility in the amorphous phase. Both the change of the amorphous phase composition and the reduced chain mobility will increase the  $T_g$ .

The  $T_g$  of the original IM bars with a high content of PA 46 (i.e., more than 50% PA 46) cannot be increased by a similar thermal treatment, because the crystallization of these blends occurs almost completely during the cooling process in the mold and cold-crystallization is suppressed. Only the blends with 30% PA 46 and less show cold-crystallization and, hence, the  $T_g$  can be increased by thermal treatment. This is given in Figure 6.

The  $T_g$  of the PA 46/PA 6I blends obtained by

solution are somewhat higher than that of the melt-processed blends. This can be ascribed to a higher degree of crystallinity of the solution-prepared blends which results in a higher concentration of PA 6I in the amorphous phase. Moreover, a higher degree of crystallinity will result in less chain mobility of the amorphous phase. Both effects will increase the  $T_g$ . It can be concluded from these experiments that transreactions between PA 46 and PA 6I will hinder crystallization of PA 46, which will be reflected in a different glass transition temperature.

#### Recrystallization During the Melting Process of Polyamide Blends

In our previous article,<sup>14</sup> it was shown that a double-melting behavior of PA 46 in the blends occurs when the blends are crystallized from the melt at high cooling rates. The double-melting behavior is due to imperfect crystals, formed during the high melt-cooling rates, which melt and recrystal-

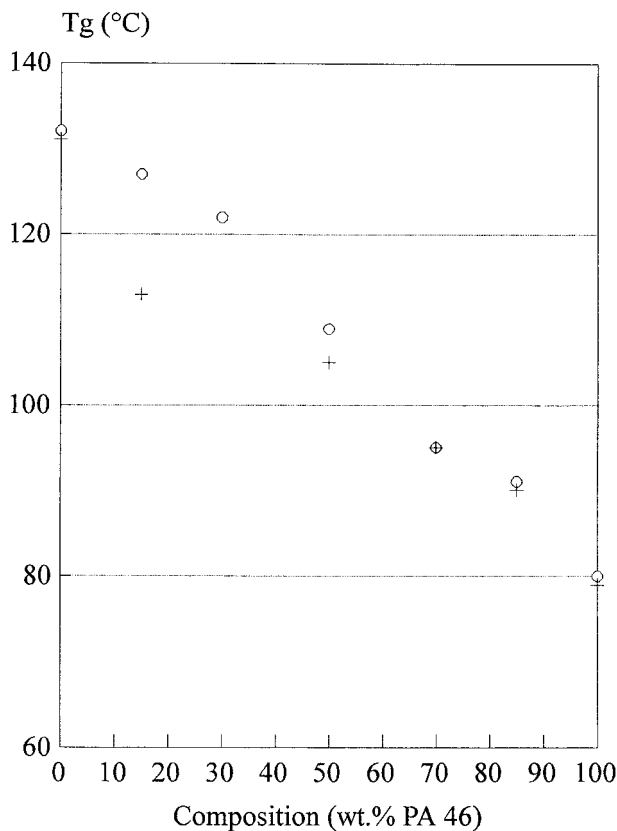


**Figure 6** Glass transition temperatures of injection-molded PA 46/PA 6I blends as a function of the blend composition: (+) original blends (cooled in the mold); (○) annealed blends.

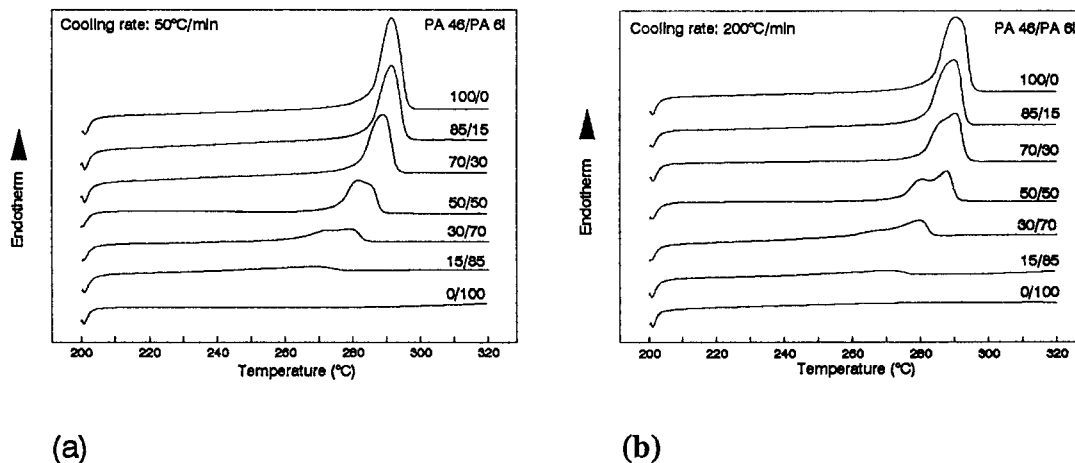


**Figure 7** Melting thermograms of the extruded PA 46/PA 6I blends obtained for various compositions after different cooling rates from the melt: (a) 50°C/min; (b) 200°C/min.

lize to more perfect crystals, and finally melt again.<sup>17</sup> It was also observed that the amount of recrystallization (i.e., the amount of imperfect crystalline structures formed) can be derived from the inverse ratio of the height of the first melting endotherm over the second one.

The recrystallization process is enhanced by higher cooling rates from the melt and also by slower crystallization kinetics of the blends at a constant cooling rate. At a cooling rate of 10°C/min, it is observed that all crystallized blend compositions show a single melting peak. However, at a cooling rate of 50°C/min, the melting endotherm of the blend composition 50/50 (w/w) starts to broaden [Fig. 7(a)]; this is the beginning of a double-melting behavior. The 30/70 blend composition already shows a double-melting behavior when the blend is cooled from the melt at 50°C/min. The melting endotherm of the 50/50 blend composition becomes a double-melting peak at a cooling rate of 200°C/min [Fig. 7(b)]. At the same cooling rate of 200°C/min, the melting endotherm of the 70/30 blend composition begins to broaden.

Previous observations can be ascribed to the different crystallization rates of the various blend compositions during the melt-cooling process. The blends which have been crystallized from the melt at low cooling rates (i.e., 10°C/min) reveal a single melting peak; rather perfect crystals are being formed at low cooling rates and thus recrystallization is suppressed. When the cooling rate is increased, compared to the crystallization kinetics of the various blends, a double-melting behavior

becomes visible; the crystalline structures which have been formed at high cooling rates from the melt can be reorganized to a higher perfection by recrystallization during the melting process of the former crystals. This double-melting behavior can also be enhanced when the crystallization rate of the blends is decreased given a constant cooling rate; this is possible by adding more PA 6I to PA 46 in the blend. However, crystallization will be hindered when the cooling rate exceeds the crystallization rate and, as a consequence, cold-crystallization will occur when these blends are heat-treated above their  $T_g$ . This was already demonstrated by quench-cooling experiments.

The inverse peak height ratio of the double-melting endotherms is, if observed, plotted against the cooling rate in Figure 8. It can be seen that the amount of recrystallization (and thus imperfect crystalline structures) increases at higher cooling rates from the melt and also with increasing weight content of PA 6I.

## CONCLUSIONS

Melt-mixing of polyamide blends using a large-scale double-screw extruder gives rise to transreaction processes resulting in the formation of copolyamides during the melt-mixing time. These transreaction processes proceed further during every melt-processing step, such as injection molding. Besides the extrusion time and the extrusion temperature, the blend composition also affects the extent of the transreaction processes.

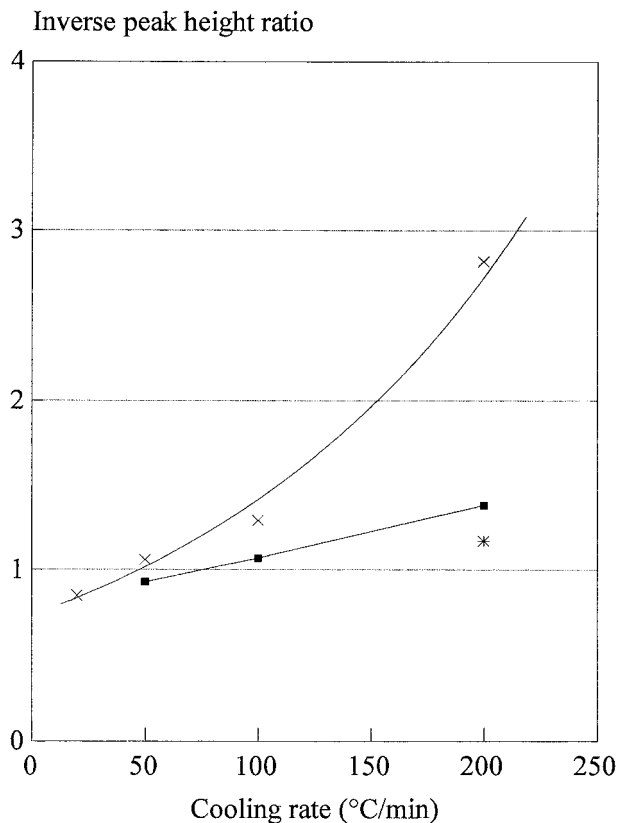


**Figure 8** Inverse ratio of the height of the first melting endotherm over the second melting endotherm as a function of the blend composition (PA46/PA6I); (\*) (70/30); (□) (50/50); (x) (30/70).

If one of the blend components is crystallizable, a large decrease in its crystallization rate is observed with an increasing amount of the noncrystallizable component. This implies the formation of imperfect crystals when these blends are crystallized from the melt at high cooling rates. These imperfect low-melting crystalline structures recrystallize into more perfect structures. If the cooling rate from the melt to room temperature

exceeds the crystallization rate, cold-crystallization becomes possible for several blend compositions when they are heat-treated above their  $T_g$ .

The authors wish to acknowledge H. Repin, R. Leeuwendal, W. Bruls, J. Van Asperen, and S. Eltink (DSM Research, Geleen, The Netherlands) for fruitful discussions.

## REFERENCES

1. M. Xanthos and S. S. Dagli, *Polym. Eng. Sci.*, **31**, 929 (1991).
2. B. K. Kim and S. J. Park, *J. Appl. Polym. Sci.*, **43**, 357 (1991).
3. R. Vankan, P. Degrée, R. Jérôme, and P. Teyssié, *Polym. Bull.*, **33**, 221 (1994).
4. C. J. Wu, J. F. Kuo, C. Y. Chen, and E. Woo, *J. Appl. Polym. Sci.*, **52**, 1695 (1994).
5. M. Kimura, G. Saleé, and R. S. Porter, *J. Appl. Polym. Sci.*, **29**, 1629 (1984).
6. J. I. Eguiazabal, M. Cortázar, and J. J. Iruin, *J. Appl. Polym. Sci.*, **42**, 489 (1991).
7. X. Yang, P. C. Painter, and M. M. Coleman, *Macromolecules*, **25**, 4996 (1992).
8. G. Montaudo, C. Puglisi, and F. Samperi, *J. Polym. Sci. Polym. Chem. Ed.*, **32**, 15 (1994).
9. H. Tobita and Y. Ohtani, *Polymer*, **33**, 2194 (1992).
10. J. G. Lertola, *J. Polym. Sci. Polym. Chem. Ed.*, **28**, 2793 (1990).
11. Y. Takeda and D. R. Paul, *Polymer*, **32**, 2771 (1991).
12. M. E. Stewart, A. J. Cox, and D. M. Naylor, *Polymer*, **34**, 4060 (1993).
13. J. Devaux, P. Godard, and J. P. Mercier, *Polym. Eng. Sci.*, **22**, 229 (1982).
14. K. L. L. Eersels and G. Groeninckx, *Polymer*, **37**, 983 (1996).
15. A. Aerdts, K. L. L. Eersels, and G. Groeninckx, *Macromolecules*, **29**, 1041 (1996).
16. K. L. L. Eersels, A. Aerdts, and G. Groeninckx, *Macromolecules*, **29**, 1046 (1996).
17. F. N. Liberti and B. Wunderlich, *J. Polym. Sci. A-2*, **6**, 833 (1968).